

Article

Investigation and Evaluation of Insolation and Ventilation Conditions of Streetscapes of Traditional Settlements in Subtropical China

Yalun Lei ¹, Hongtao Zhou ^{1,*} , Qingqing Li ², Yigang Liu ², Ji Li ³ and Chuan Wang ⁴

¹ College of Design and Innovation, Tongji University, Shanghai 200092, China; 22310129@tongji.edu.cn

² College of Art and Design, Nanjing Forestry University, Nanjing 210037, China; jiangzhishu@njfu.edu.cn (Q.L.); neal_liu@njfu.edu.cn (Y.L.)

³ College of Art and Design, Nanjing Vocational University of Industry Technology, Nanjing 210023, China; moonlight202106@126.com

⁴ School of Design and Fashion, Zhejiang University of Science and Technology, Hangzhou 310023, China; wangdachuan3781@gmail.com

* Correspondence: zhouhongtao@tongji.edu.cn; Tel.: +86-186-0055-0496

Abstract: Global warming, the urban heat island effect (UHI), and the risks of fossil fuel depletion necessitate a re-evaluation of traditional settlements that have been adapted to local climatic conditions, topography, and available resources, including materials and construction methods, through passive strategies to achieve thermal comfort. Although vernacular settlements have received considerable attention, few have examined and evaluated their streetscapes. This study investigates the impact of topographical features and architectural forms on insolation and ventilation conditions in traditional settlements in China's southern subtropical climate. The aim is to explore traditional planning configurations of streetscapes at different altitudes to identify architectural forms and planning strategies that effectively improve outdoor users' thermal comfort conditions. For this purpose, case studies are conducted on three traditional settlements in Lingnan; the Lingnan region has a typical subtropical climate in southern China. The chosen cases represent the main features of different topographical conditions, architectural forms, and climate zones in the Lingnan. We systematically simulated the insolation and ventilation in these settlements' streetscapes on a monthly and quarterly basis and analyzed their sunlight hours, incident solar radiation, shading percentages, sky view factors (SVF), and wind speed. The findings show the following: (1) Specific terrains can affect streetscapes' shading percentages and wind speed. The mountain settlement (With an average elevation of 600 m) is located on a southeast-facing slope ($10^\circ < \text{slope} < 20^\circ$). It receives an additional 10% of incident solar radiation compared to gentle terrain. (2) Compared to settlements located in coastal hills and mountainous, plain settlements have better shading and ventilation conditions in streetscapes. In terms of insolation, plain settlements have denser building configurations and narrower, elongated street corridors with a height-to-width ratio (H/W) = 1.9~5.5 (the height-width ratio value as street's H/W (H = height, W = width); note that it is unitless), which can generate greater lower SVF (44.5%), and shading percentages (63.6%). Regarding ventilation, it is easier to create a "cool lane" (i) when the main street, oriented towards the dominant wind direction in summer, forms an angle $< 30^\circ$ with it, (ii) when the primary street follows a NE-SW longitudinal orientation, while SE-NW horizontal streets intersect and weave through it, and (iii) with a H/W = 3~4 resulting in wind speeds of 2.9~4.0 m/s. (3) All the streetscapes have overshadowing occurring in winter; similarly, varying sizes of calm wind zones are created in summer. To alleviate these issues, widening the streetscapes along the buildings can permit solar penetration and natural ventilation. (4) In summer, installing shading devices along the horizontal plane of covered street corridors with a H/W = 1~4 and N-S longitudinal orientation can provide an additional shading of 3.6~22%.

Keywords: traditional settlements; climate-adaptive design; the subtropical climate; streetscapes; insolation and ventilation condition; topographical features



Citation: Lei, Y.; Zhou, H.; Li, Q.; Liu, Y.; Li, J.; Wang, C. Investigation and Evaluation of Insolation and Ventilation Conditions of Streetscapes of Traditional Settlements in Subtropical China. *Buildings* **2023**, *13*, 1611. <https://doi.org/10.3390/buildings13071611>

Academic Editor: Samira Garshasbi

Received: 19 May 2023

Revised: 22 June 2023

Accepted: 23 June 2023

Published: 26 June 2023



Copyright: © 2023 by the authors. Licensee MDPI, Basel, Switzerland. This article is an open access article distributed under the terms and conditions of the Creative Commons Attribution (CC BY) license (<https://creativecommons.org/licenses/by/4.0/>).

1. Introduction

1.1. Background and Objectives

In recent years, the increasing urbanization rate and the impact of industrialization have led to the construction of modern and standardized buildings in both urban and rural areas, aiming to provide residents with convenient and comfortable contemporary lifestyles. However, this development comes at the cost of high energy consumption [1]. The construction industry accounts for approximately 40% of global energy consumption, 36% of carbon dioxide (CO₂) emissions, and 50% of the electricity demand [2,3]. In 2018, the total carbon emissions of buildings accounted for 51.2% of China's energy carbon emissions [4]. To achieve the international goal of net-zero emissions by 2050 [5,6], it is urgent that we improve the energy efficiency of buildings and reduce their negative impact on the environment. The buildings' energy efficiency can be enhanced through design strategies that incorporate green streetscapes connecting indoor and outdoor areas [7]. It is generally accepted that vernacular architecture adapts to local climatic and socio-cultural features with traditional techniques and available materials, and achieves a thermally comfortable outdoor environment with low energy consumption through the incorporation of passive design approaches [8,9]. The present study introduces a comparative investigation and evaluation of insolation and ventilation conditions for traditional settlements' streetscapes in different topographical and climatic zones of the Lingnan region, located in southern China, with a typical subtropical climate. The goal is to showcase the potential of transforming traditional passive design approaches into modern urban-outdoor-space climate-responsive design strategies and environmental policy drafting, specifically targeting the specific climatic and topographical characteristics of a region.

1.2. Literature Review

The climate-responsive design is one of the specialized concepts and strategies for dealing with global warming and UHI [10]. Thermal comfort is usually defined as "that condition of mind that expresses satisfaction with the thermal environment", and the provision of comfort indoors is a fundamental objective of architects, engineers, and the allied building sector professions [11]. According to Wenting Yang et al., the climate-responsive design concept refers to architectural design that is adapted to specific local climates and natural environmental conditions [12,13]. According to Mobark M. Osman et al., the climate-responsive design is defined in terms of spatial planning that provides thermal comfort for occupants while reducing energy consumption [14]. According to Yan Du, architects can create a healthy and comfortable indoor and outdoor microclimate without relying on heating, ventilation, and air conditioning systems (HVACs) [15]. The first step in energy-efficient building design is to adapt to the climate through passive design techniques [16]. Therefore, climate-responsive design involves adapting buildings to their specific climatic conditions through passive strategies before resorting to active solutions [14]. This approach aims to create thermal comfort in indoor and outdoor environments, leading to reduced energy consumption, CO₂ emissions, and lower UHI, and contributing to the mitigation of global warming [17].

Research on streets, especially green streets, can be regarded as a sustainable approach to a linear public outdoor space that may form a part of connecting urban green grids [18,19]. It is widely recognized that traditional settlements' streets play a crucial role in influencing the energy consumption of buildings. If properly designed, this street model based on passive strategies can mitigate negative environmental impacts and provide thermal comfort and favorable microclimate conditions in a low-energy manner [20]. According to Yongxin Xie et al., solar radiation and wind speed are the key parameters affecting the thermal comfort of pedestrians in outdoor spaces in hot-humid climate regions [21]. Some previous studies have confirmed the correlation between outdoor space microclimate environment and building density, street morphology, greenery arrangement, pavement materials, and shading devices [8,12,22]. More specifically, the morphology of buildings on both sides of the streets, street width, building height on both sides of the street, and the texture of

the surrounding area are all factors that contribute to streetscapes' formation [23]. Among these factors, the street's orientation and H/W significantly impact the microclimate environment of the streetscape [24]. However, research results in different regions have shown some variations.

Regarding the street corridor layout, there is evidence that deep street corridors work better in improving outdoor thermal comfort than shallow street configurations in hot-humid regions. Yunfang Jiang et al. notes that continuous long-narrow street corridors can have a significant cooling effect, forming "cool lanes" during extreme daytime heat hours in summer [19]. In contrast, during field measurements in shallow streets, higher temperatures are observed because these streets are more exposed to solar exposure. Some studies have found that, as the SVF value decreases, the duration of solar exposure decreases, resulting in larger shaded areas and better cooling effects during the day [25]. This is because SVF determines the value of thermal radiation exchange between the outdoor space and the sky during the day, which influences the degree of temperature fluctuation, whether it be lower or higher [26]. Regarding wind performance, the natural ventilation and insolation in street corridors are not correlated. Xuemei Han et al. proves that the natural ventilation in street corridors was better when the build-to-line ratio was similar to the H/W and had low SVF [27]. It is worth noting that narrow and unconnected street corridors also reduce the ventilation of the internal space within settlements [28]. For example, static wind zones are often found in the interior spaces of densely networked streets [29].

Building density is another factor that affects outdoor thermal comfort. On sweltering summer days, a compact building layout is more effective in reducing temperatures than an open building layout [30]. For example, Yingjie Jiang et al. conducted a study on the impact of different public-space-planning schemes on outdoor thermal comfort for pedestrians in the city of Wuhan. They found that street corridors located in open areas were more susceptible to high temperatures than those in dense areas [31]. Galal, O.M. et al. conducted measurements of shading patterns and on-site air temperatures in two sites located in New Aswan, Egypt [32]: the first site is situated in a dispersed modern urban area, while the second site is found in a compact traditional urban area. The results revealed that the second site consistently had lower temperature recordings during the summer.

In addition to the architectural environment, the natural environment and local topography also influence the passive design concepts of insolation and ventilation [33]. Topographical characteristics not only affect a settlement's scale but also impact the individual street's thermal comfort [34]. According to Hermawan, variations in elevation are the most significant factor influencing the traditional settlements' outdoor microclimate conditions [35]. Xiong et al. assessed the Jiangnan traditional villages in China's subtropical climate zone and inferred that their overall spatial layout conforms to the ideal model of "Feng Shui" in Chinese culture [8]. These villages are surrounded by mountains on both the east and west sides, with the latter being closer to the village outskirts. During winter, the western mountains act as a barrier against the monsoon winds, reducing their impact on the village. The eastern side of the hill is further away from the village's edge, creating a wide expanse of flat farmland as a barrier between the villages, providing a gyratory space for the summer monsoon and facilitating ventilation and heat dissipation. A meandering water system to the east and a large body of water to the south increase the village's humidity and assist the farmland's irrigation. These waters also promote living and production, while creating a favorable microclimate.

On the one hand, this overview points to a strong relationship between topographical characteristics, street corridor layout, building density, and outdoor thermal comfort, and the insolation and ventilation; and, on the other hand, a review of the relevant literature shows that compact urban layouts, long-narrow street corridors with traditional architectural features, and the settlements' overall spatial pattern in synergy with the natural environment and local topographical features can have the effect of improving outdoor thermal comfort. The methods used in the above studies are based on qualitative and quantitative results obtained from on-site observations, topographic map analysis, field

measurements, and simulation studies. Comparative analysis methods have also been used to demonstrate the thermal comfort conditions of different built forms and massings between specific urban old and new districts; however, there is still a limited amount of literature available on the comparative evaluation of climate-responsive design in traditional settlements' streetscapes under different topographies, climate regions, and spatial planning configurations.

2. Materials and Methods

First, based on this study's purposes, specific standards are set for three representative traditional settlement selections for comparative analysis. Second, the topographic features, building forms, and streetscape characteristics of selected traditional settlements are investigated by examining topographic maps, wind field simulation and spatial pattern maps, aerial photographs, field measurements, and meteorological data (the meteorological data in these settlements have been obtained from the National Meteorological Science Data Center, China). Third, the research conducted a series of calculations and data visualization to assess and evaluate various variables related to thermal comfort in streetscapes. These variables include sunlight hours, incident solar radiation, shading percentage, SVF, H/W, and wind speed. Fourth, we introduce the research significance and reveal the passive design approaches embedded in it, and explore the future works of climate-adaptive design in urban outdoor spaces.

2.1. Selection Criteria

For the goals of this study, three representative traditional settlements located in the Lingnan region were selected for comparative evaluation (Figure 1). The standards set for these traditional settlements in this study are as follows: (i) There are distinctive traditional architectural features and are relatively well-preserved. (ii) They have representative climatic conditions, topographies, and landscape configurations, including mountains, plains, and coastal hills. (iii) The settlements' overall spatial layout and streetscapes can represent the characteristics of Lingnan traditional settlements.

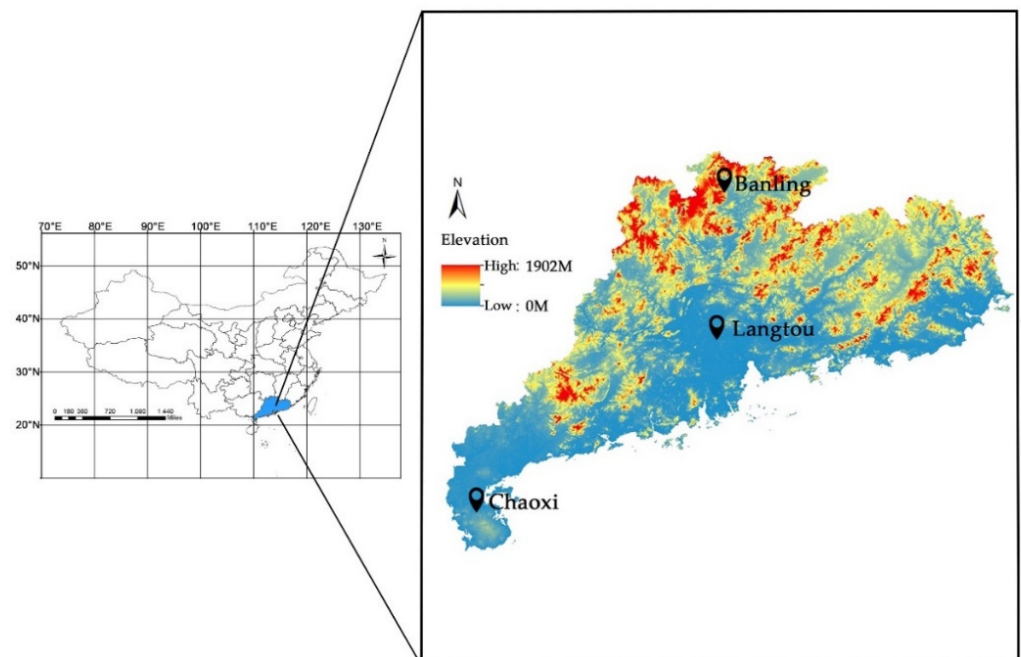


Figure 1. Map of Lingnan indicating the three traditional settlements under study relative to the topography.

2.2. Mapping of Insolation Conditions

First, using the Relative Geo-location tool in SketchUp Pro 2021 software, we can connect to satellite maps (such as Google Earth, 2022) to generate a 3D model of the terrain of a sample settlement. Second, to improve computational efficiency, this study used AutoCAD 2022 to depict the settlement layout plans and then imported the CAD plan into 3DMAXS 2020 to build the geometric models of buildings and streets, based on the feasibility of previous experimental methods, combined with data from the site surveys, relevant research literature, and Google satellite maps (4K UHD). Third, elevation and slope recognition of the terrain is accomplished using the “Color by slope” plugin within SketchUp Pro 2021 software. After that, the topographic and architectural digital models were imported into the environmental simulation software Ecotect-Analysis 2011.

Ecotect is a 3D environmental simulation program that is widely used by scholars to simulate energy efficiency under various climate conditions, including solar radiation, day-lighting, and thermal comfort, with passive design as a concept [36]. The simulation results obtained using Ecotect are known for their accuracy, efficiency, and visual responsiveness. The specific experimental steps are as follows:

1. Computational domain and grid.

According to the “Chinese Lighting Design Standard” [37], based on the light and climate zones, offset the 2D Slice positions by 0.6 m along the Y-axis. Based on the principle of building density and staying as square as possible, set the grid size for BanLing (T1) as follows: Grid Size, 102 m × 212 m × 0.2 m; Number of Cells, 1.2 m × 1.2 m × 1.2 m. Set Langtou (T2) as follows: Grid Size, 192 m × 272 m × 2.8 m; Number of Cells 0.6 m × 0.6 m × 0.6 m. Set Chaoxi (T3) as follows: Grid Size 335 × 430 × 2.8 m; Number of Cells 0.8 m × 0.8 m × 0.8 m.

2. Light environment settings.

First, we load the corresponding meteorological data (in .wea format) based on the meteorological characteristics of the settlement’s location. The meteorological data were obtained from “the Special Meteorological Dataset for Building Thermal Environment Analysis in China” [38,39]. Then, select “calculate < lighting analysis < natural light levels-daylight factors-levels” mode and turn on the high precision and “CIE Overcast Sky” (4500 lux) calculation models, and “Calculate Over for the Analysis Grid”. Finally, based on these settings, the software can calculate the monthly values of incident solar radiation on different terrain surfaces and mappings of total average daily sunlight hours for each quarter and month. It also generates the mapping of SVF and sunlight hours on the horizontal surface of the streetscapes and the monthly statistical table of shading percentage and insolation.

Furthermore, the calculation of incident solar radiation data and mappings is based on the monthly values of incident solar radiation from 08:00–18:00 in the representative traditional settlements. Insolation simulations are to identify the solar characteristics of different terrain and spatial forms’ planning configuration. The contour lines between varying street corridors in the SVF mappings use different colors to mark SVF values, indicating the level of the sky exposed along the street corridors. For example, the red color shows a region with 100% exposure to the sky, while blue indicates a part with 0% sky exposure. In other words, red plays a region with a low-stable thermal environment, while blue shows an area with a high-stable thermal environment. Based on the 3D models of the terrain and building massing, generate mappings of average daily values of sunlight hours between 08:00 and 18:00 during summer and winter. Different colors are used between the contour lines in the sunlight hours mapping to mark the corresponding sunlight hours, thus distinguishing between insolation and shaded portions. For example, yellow and blue colors present two poles, yellow presenting the part of streetscapes where the sun can penetrate, and blue indicates the obscured streetscapes. Finally, the monthly average shading percentage distributions throughout the year and the shading are calculated. Shading simulations also assess the streetscapes with shade facilities during the summer.

2.3. Mapping of Ventilation Conditions

The Computational Fluid Dynamics (CFD) software Phoenix 2019 was used to simulate the natural ventilation of representative traditional settlements. Phoenix is currently the leading CFD analysis software and its “flair specialization module” has been widely used by many researchers to simulate buildings’ wind environments at different scales, and the accuracy of its calculation results has been well-proven [40]. The numerical simulation process can be divided into geometric modeling, determination of the control equations, construction of the computational domain and mesh generation, natural wind boundary condition setting, and post-processing operations.

1. Geometric modeling. Due to the real mountain models with numerous curved surfaces, it can be challenging for computers to handle them. About previous experimental methods [41], the DEM data need to be converted into contour lines using the “Intersect Faces” command in SketchUp Pro 2021 software. This allows for the creation of a new sandbox to work with. Based on the complexity of the terrain, the simplification of the Banling (T1) model adopts an 80 m contour interval, while the simplification of the Langtou (T2) and Chaoxi (T3) models adopts contour intervals of 1 m and 5 m, respectively.
2. Determination of the control equations. Considering that the airflow around the building is generally incompressible and has low-velocity turbulent flow, in line with Boussinesq assumptions [42], the contact between the airflow and the building forms a restricted flow. The standard RNG $k-\epsilon$ model has better results for restricted flow (with wall constraints) and has the advantages of low computational cost and relatively accurate predictions. Therefore, it is widely used.
3. Construction of the computational domain and mesh generation. According to the calculation region range recommended by Xiaoyu Ying et al. [43], the model should be set with a longitudinal (x) extent of 5 times, a transverse (y) extent of 5 times, and a vertical (z) extent of 3 times. The positive Y-axis direction should be set as the north direction. As the mountain is a simplified surface with an extremely irregular shape, this paper adopts an unstructured grid that is employed for mesh partitioning, and local refinement is applied to the grid in the area where the building is located.
4. Natural wind boundary condition setting and post-processing operations (Table 1).
 - (i) Selection of different boundary layers according to the natural environment features, “the Design code for heating ventilation and air conditioning of civil buildings” (GB50736-2012, China), and the on-site wind conditions through which the settlement winds mainly pass [44].
 - (ii) The outdoor wind at a pedestrian height of 1.5 m is adopted. Since the gradient wind at the site varies with the height of the building, the profile type operation rate is chosen as a power law, with a power law index of 0.14 (based on wind pressure height variation factor).
 - (iii) Set the dominant wind direction, wind speed, and temperature for summer and winter in Chaoxi (T3), Langtou (T2), and Banling (T1). The velocity contour mapping of the street corridors is marked with a different color. For example, red represents a high-wind-speed area, while blue represents a low-wind-speed area. The convergence residuals for velocity, momentum, and turbulence kinetic energy should be set to be below 10^{−4}. However, if the convergence of the continuity equation is poor, the criterion can be relaxed to 10^{−3} [43,45]. Based on Soligo’s findings on comfort wind speed and frequency under different conditions [46], as well as the research by Murakami et al., which introduced the outdoor comfort wind range under different temperature ranges [47], it has been determined that the comfortable wind speed for the Lingnan region in summer is 0.7–5.0 m/s. The calm wind speed is 0–0.5 m/s, and wind speeds >5.0 m/s are considered uncomfortable.

Table 1. Natural wind boundary condition setting.

	Banling (T1)	Langtou (T2)	Chaoxi (T3)
Topographic calculation domain size	17,385 m × 19,625 m × 2400 m	4515 m × 5685 m × 45 m	6310 m × 6660 m × 125 m
Building calculation domain size	450 m × 1100 m × 24 m	1950 m × 2200 m × 30 m	1930 m × 2240 m × 24 m
Summer wind direction & average wind speed	Southeast, wind speed 7.0 m/s	Southeast, wind speed 1.9 m/s	Southwest, wind speed 3.4 m/s
Winter wind direction & average wind speed	Northeast, wind speed 6.5 m/s	Northwest, wind speed 2.05 m/s	Northwest, wind speed 4.6 m/s
Daily maximum temperature	39°	37°	38°
Select terrain type & effective roughness height	Type = C; $\alpha = 0.75$	Type = B; $\alpha = 0.1$	Type = B; $\alpha = 0.1$
Total number of iterations	1000	500	500

3. Results

3.1. Selection of Settlements

Banling (T1) is located in Ruyuan Country in northern Guangdong Province (at 24°28' N and 112°52' E), with an average altitude of 600 m, and is a typical Yao traditional settlement (Figure 1). The topographic map (Figure 2A, Table 2) shows that the settlement lies at a hillside, and buildings spread out along the contour lines, forming closely connected buildings and long-narrow street corridors. Most of the buildings show a linear configuration. Due to the high altitude, this area is relatively cold in winter (Figure 3). There are mostly S–E winds in summer, and an N–W monsoon prevails in winter (Table 1).

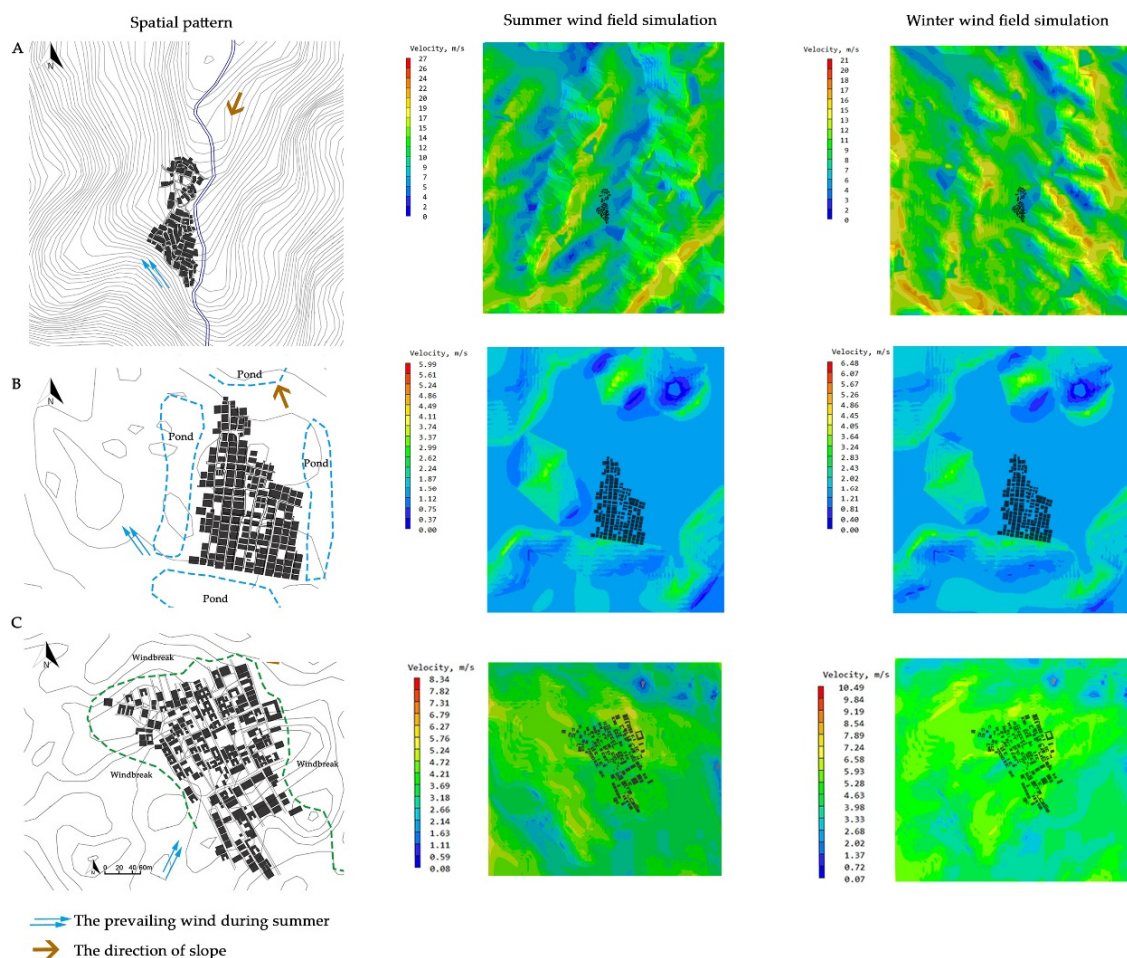


Figure 2. Wind field simulation and spatial pattern map of (A) Banling (T1), (B) Langtou (T2), and (C) Chaoxi (T3).

Table 2. Natural and man-made characteristics of the three traditional settlements under study.

	Banling	Langtou	Chaoxi
Topography	N–E-facing steep slope (T1)—Mountainous regions	Flat terrain (T2)—Plains regions	A concave gentle slope (T3)—Coastal hills regions
Spatial Layout of the Settlement	Linear with narrow facades (compact)	Comb-like spatial layout (compact)	Comb-like spatial layout (semi-dispersed)
Building Form	Linear or U-shaped	Linear with narrow facades	Linear or U-shaped
Building Stories	Single-story, double-story	Single-story, double-story	Single-story
Street Orientation	N–S axis, SE–NW axis	NE–SW axis, SE–NW axis	NW–SE axis, SW–NE axis
H/W	1.9–4.8	1.9–5.5	0.9–2.3
Open Spaces	Small courtyards	Small courtyards	Large courtyards

Langtou (T2) is located on a plain with a dense network of rivers (at 23°24' N and 113°13' E), with an average elevation of 3 M (Figure 1). Figure 2B shows that the overall spatial layout of Langtou (T2) is neatly arranged, with buildings tightly connected in a typical comb-like spatial layout. (The majority of architectural floor plans are designed in the style of a U-shaped configuration, with each courtyard arranged in a N–S orientation in the shape of a comb, forming rows of buildings. Each courtyard is nested within another courtyard.) There are vast fields and large fish ponds in the settlement's front, and the long-narrow NE–SW longitudinal street corridors are perpendicular to the fish ponds. The narrow corridor between two rows of buildings, commonly known as "Li" or formerly referred to as a "fire corridor", is the main transportation street corridor within the traditional settlement. One can discover certain streetscapes equipped with shading devices along this street corridor. The southern side of the settlement is far from the northern side; a transverse transportation street corridor was established to connect the SE–NW. The buildings within Langtou (T2) are mostly one-or-two-story high, with a compact layout, towering building walls, and a "U" courtyard shape (small-scale courtyards), resulting in a more concentrated building layout and street corridors (Table 2). This region has long summers and short winters, with hot-humid summers and warm winters (Figure 3), and S–E winds in summer and N–W winds in winter (Table 1).

Chaoxi (T3) is located in the coastal hilly area of Leizhou Peninsula (at 20°43' N and 110°05' E), facing the mainland to the north and bordered by the sea on three sides, with an average elevation of 38 m (Figure 1). Chaoxi (T3) also has a comb-like layout, but it is not as straight and neat as observed in Langtou (T2). Compared with Langtou (T2), Chaoxi (T3) has a more significant number of E–W street corridors and higher H/W, breaking the comb-like spatial layout to some extent. Most of the buildings here have semi-enclosed spaces and are primarily one-story high (Table 2). Since this area is located in the transitional climate zone between the tropics and the subtropics, it is characterized by hot and long-lasting summers and warm winters (Figure 3). The S–E winds prevail throughout the year, with more S–W winds in summer and N–W winds in winter (Table 1).

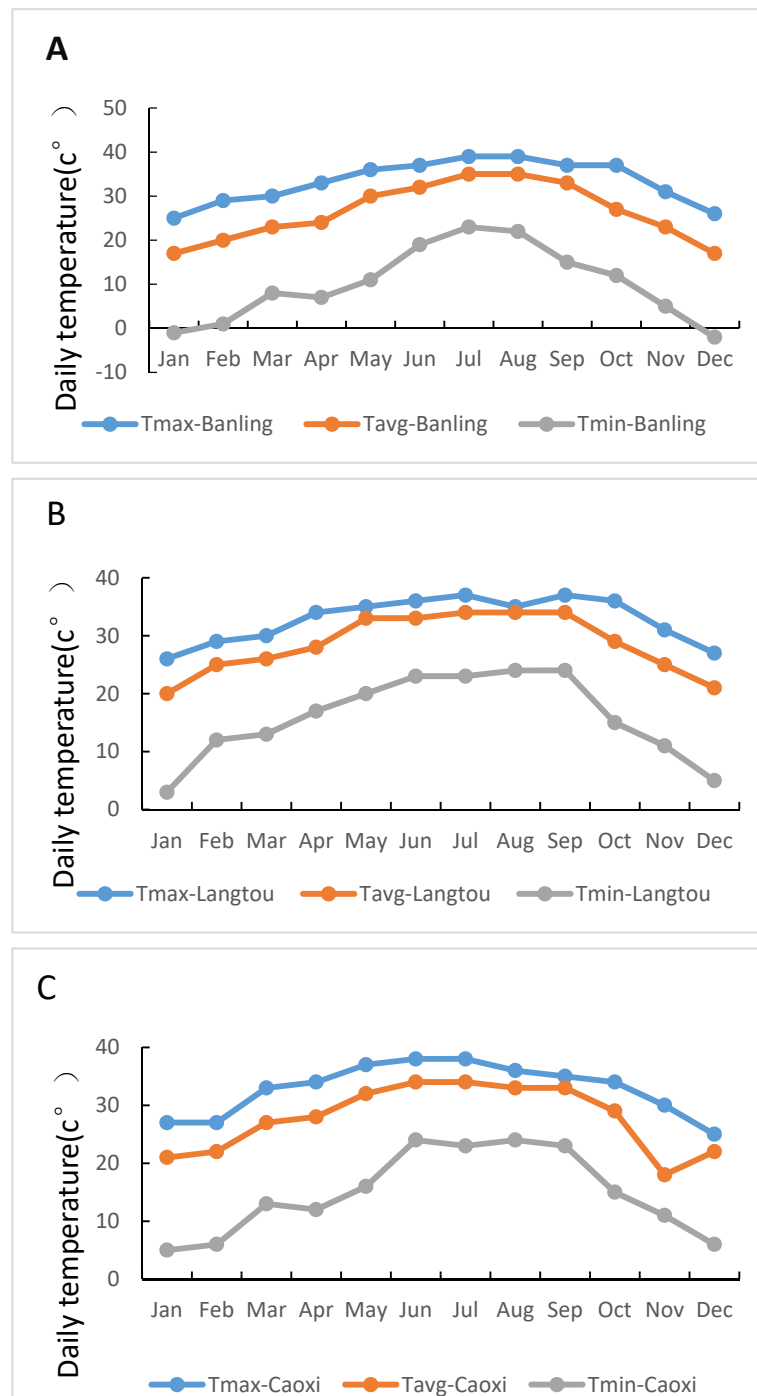


Figure 3. Minimum, mean, and maximum air temperature for (A) Banling (T1), (B) Langtou (T2), and (C) Chaoxi (T3). Source: National Meteorological Science Data Center, China.

3.2. The Environmental Impact of Topographical Features

The wind field simulation and spatial pattern map shows (Figure 2A) that Banling (T1) has low wind speeds in winter as it is located on the southeast slope of the river valley, surrounded by mountains on three sides, with the western side closely adjacent to the mountain. The settlement is open to the east and south, and at a distance from the hills to the east, so that the summer winds can follow the slope and enter the settlement without much influence on the wind speed. According to the calculations based on monthly and quarterly incident solar radiation data in the settlement's different directions (Table 3), we found that the settlement takes advantage of the lower solar angles and south-facing exposure, creating

favorable sunlight conditions during the winter. Compared to the relatively gentle slopes in the northern, western, and southern directions, the southeast-inclined terrain receives more incident solar radiation due to its orientation. More specifically, in winter, the southeast, west, south, east, north, and flat regions distributed at slopes of 10° – 20° have a cumulative incident solar radiation of 180.94 MJ/m^2 , 159.55 MJ/m^2 , 178.20 MJ/m^2 , 181.87 MJ/m^2 , 177.44 MJ/m^2 , and 85.10 MJ/m^2 , respectively. The incident solar radiation in the southeast direction has increased by 10% compared to the flat terrain. In addition, mountainous terrain significantly impacts building massing configurations and street corridor planning in Banling (T1). Due to the topographical constraints and lack of available space, buildings develop upwards, resulting in a long-narrow street corridor ($H/W = 1.9\text{--}4.8$) and a more compact building layout (Table 2).

Table 3. Mean monthly and mean seasonal incident solar radiation for the flat surface of Banling (T1) and for surface tilted by $20\text{--}30^{\circ}$ for southeast, west, south, east, north, and flat.

Incident Solar Radiation (MJ/m^2)						
Month/Surface	Southeast	West	South	East	North	Flat
June	347.15	299.76	325.42	338.48	336.25	1586
July	412.57	370.88	379.09	428.04	422.64	184.98
Aug	398.17	337.46	345.35	389.89	381.68	175.43
Summer	385.92	336.06	349.99	385.56	380.29	172.80
Dec	223.32	193.12	220.15	230.59	213.52	102.53
Jan	165.32	149.99	162.91	163.15	165.38	78.87
Feb	154.13	135.61	151.57	151.88	153.52	73.94
Winter	180.94	159.55	178.20	181.87	177.44	85.10
Mar	153.69	136.15	151.64	150.24	153.55	73.01
Apr	220.15	195.35	217.13	214.1	218.45	106.45
May	304.63	265.43	300.06	295.5	300.86	142.42
Spring	226.15	198.97	222.95	219.96	224.28	107.28
Sept	356.05	303.88	349.31	352.19	351.26	157.54
Oct	297.32	256.19	292.72	295.88	293.44	137.09
Nov	255.86	209.82	253.40	269	248.51	109.45
Autumn	303.08	256.58	298.48	305.68	297.72	134.68

As shown in the wind field simulation and spatial pattern map (Figure 2B), we find that the plain river network plays a fundamental role in the “comb-like spatial layout” and landscape configuration of Longtou (T2): (i) The settlement is located in the north, facing south, and is built along the slope with a low front and higher back. (ii) In front of the settlement are vast fields and large fish ponds, surrounded by trees to the north. The wind blows from the fields in front of the settlement and enters the public outdoor space through the street corridors ($H/W = 1.9\text{--}5.5$, orientated NE–SW) and the “U” courtyard during summer, while the wind is blocked by the tall trees in the north during winter (Table 2). Although the settlement’s topography has a certain inclination, the inclination of the surrounding terrain is $\leq 10^{\circ}$, which has little effect on the incident solar radiation on the surface in different directions. The simulated cumulative incident solar radiation values in the different settlement directions were $91.12 \text{ MJ/m}^2\text{--}91.74 \text{ MJ/m}^2$ in winter and $123.16 \text{ MJ/m}^2\text{--}124.51 \text{ MJ/m}^2$ in summer.

According to the wind field simulation and spatial pattern map (Figure 2C), Chaoxi (T3) is located in a low-lying hilly area along the coast, with a gradual slope from N~S (Figure 1). The overall gradient is $\leq 10^{\circ}$. Winter’s maximum accumulated incident solar radiation value occurs in the central part with the most considerable inclination angle (733.60 MJ/m^2), and the minimum in the southern region with a flat inclination (670.71 MJ/m^2). In summer, the accumulated incident solar radiation values on different surface orientations in the settlement exhibit minimal changes ($1158.16 \text{ MJ/m}^2\text{--}1166.94 \text{ MJ/m}^2$). The settlement experiences higher wind speeds during the summer, especially on the west ($5.2 \text{ m/s}\text{--}6.3 \text{ m/s}$) and northeast sides ($5.8 \text{ m/s}\text{--}7.3 \text{ m/s}$). The settlement has a circular

pond located to the southeast as an opening, while tall trees surrounded the other direction. During the summer, the prevailing wind can be introduced to the settlement's front buildings through the pond's opening. To withstand typhoons and facilitate drainage, the buildings are designed with specific considerations. Firstly, the spatial layout of the buildings is relatively open, avoiding the presence of continuous long-narrow streets ($H/W = 0.9\sim 2.3$). Additionally, the buildings are designed with a lower front and higher back, gradually increasing in elevation. This design approach promotes optimal storm resistance and effective drainage. However, in summer, this planning configuration can lead to ineffective shading in the streetscape and difficulty in creating "cool lanes" (Table 4).

3.3. Environmental Explanation of Streetscapes Based on SVF and Sunlight Hours

Analysis of SVF mappings in Banling (T1) shows that the low SVF values ranging from 0.01~0.20 and 0.21~0.40 account for 8.8% and 35.7% of the streetscape area, respectively (Table 5, Figure 4). (SVF represents the proportion of visible sky from the ground and is closely related to the amount of solar radiation received on a horizontal plane. SVF is a dimensionless quantity ranging between 0 and 1, where a value of 1 indicates that the sky is completely visible. When there are buildings or trees surrounding the measurement point, the SVF will be proportionally reduced.) The lower SVF values are a result of the shading caused by the long-narrow, variable street layout, and the interweaving of buildings within the area. The SVF values ranging from 0.41~0.50 and 0.51~0.60, respectively, account for 19.5% and 14.2% of the area of street corridors, respectively. The higher SVF values result from several factors, including low-rise buildings, loose street corridors, and undulating mountainous terrain that enhance the visibility of streetscapes. Regarding sunlight hours, insolation simulations indicate that most of the streetscapes in Banling (T1) can avoid being affected by intense solar radiation, with a shading rate of 63.6%. In contrast, in winter, the streetscapes' shading rate is too high, accounting for 85.7% (Table 4, Figure 5).

Table 4. Percentage of the street area with predominantly sunny and shady conditions for wintertime and summertime for the three settlements under study.

Insolation Conditions (%)			
	Banling (T1)	Langtou (T2)	Chaoxi (T3)
Summer			
sunny	36.4	37.6	71.6
shady	63.6	62.4	28.4
Winter			
sunny	14.3	25.3	50.5
shady	85.7	74.7	49.5

Table 5. Sky view factor mappings of streets for the three settlements under study.

Sky View Factor Distribution (%)			
	Banling (T1)	Langtou (T2)	Chaoxi (T3)
0.01–0.10	1.4	7.1	2.0
0.10–0.20	7.4	12.9	0.9
0.21–0.30	14.4	23.2	2.0
0.31–0.40	21.3	19.7	3.3
0.41–0.50	19.5	16.2	6.6
0.51–0.60	14.2	10.1	12.0
0.61–0.70	7.3	5.6	16.0
0.71–0.80	7.8	4.2	18.2
0.81–0.90	4.9	1.1	16.2
0.91–1	1.8	0	15.6

Sky View Factor Mappings

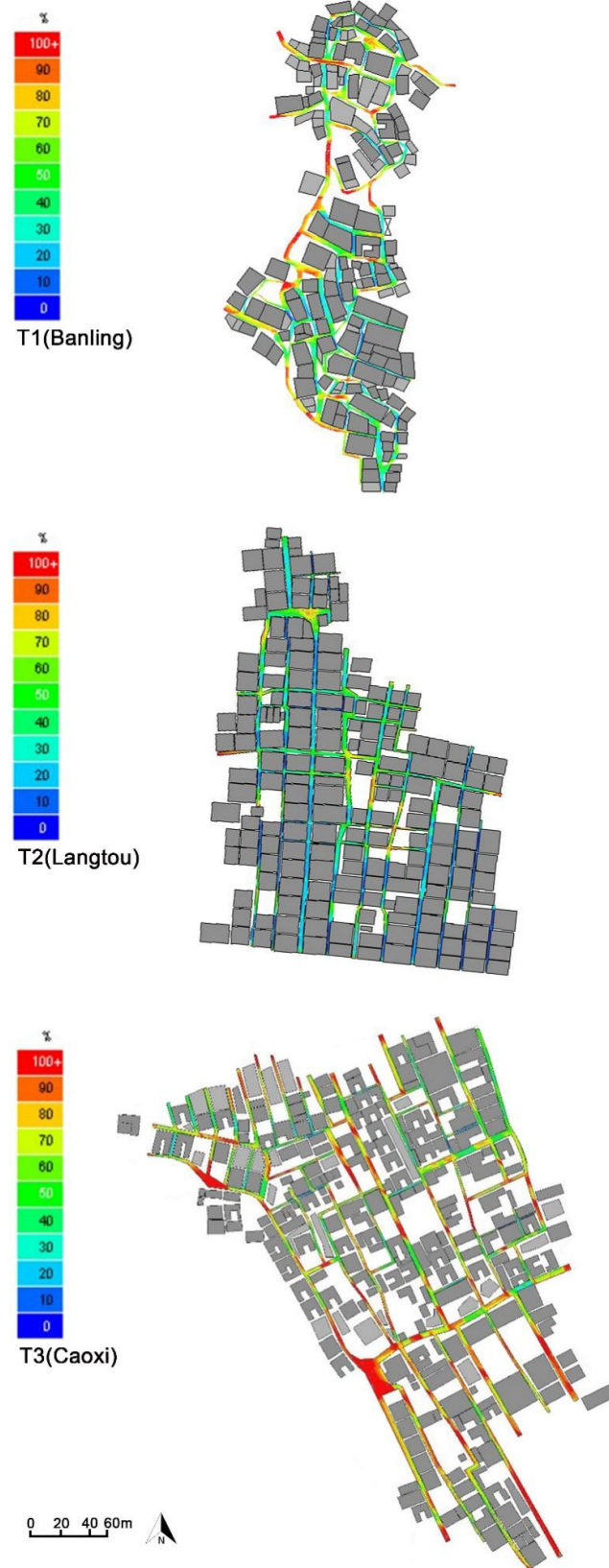


Figure 4. SVF of streets for the three traditional settlements under study.

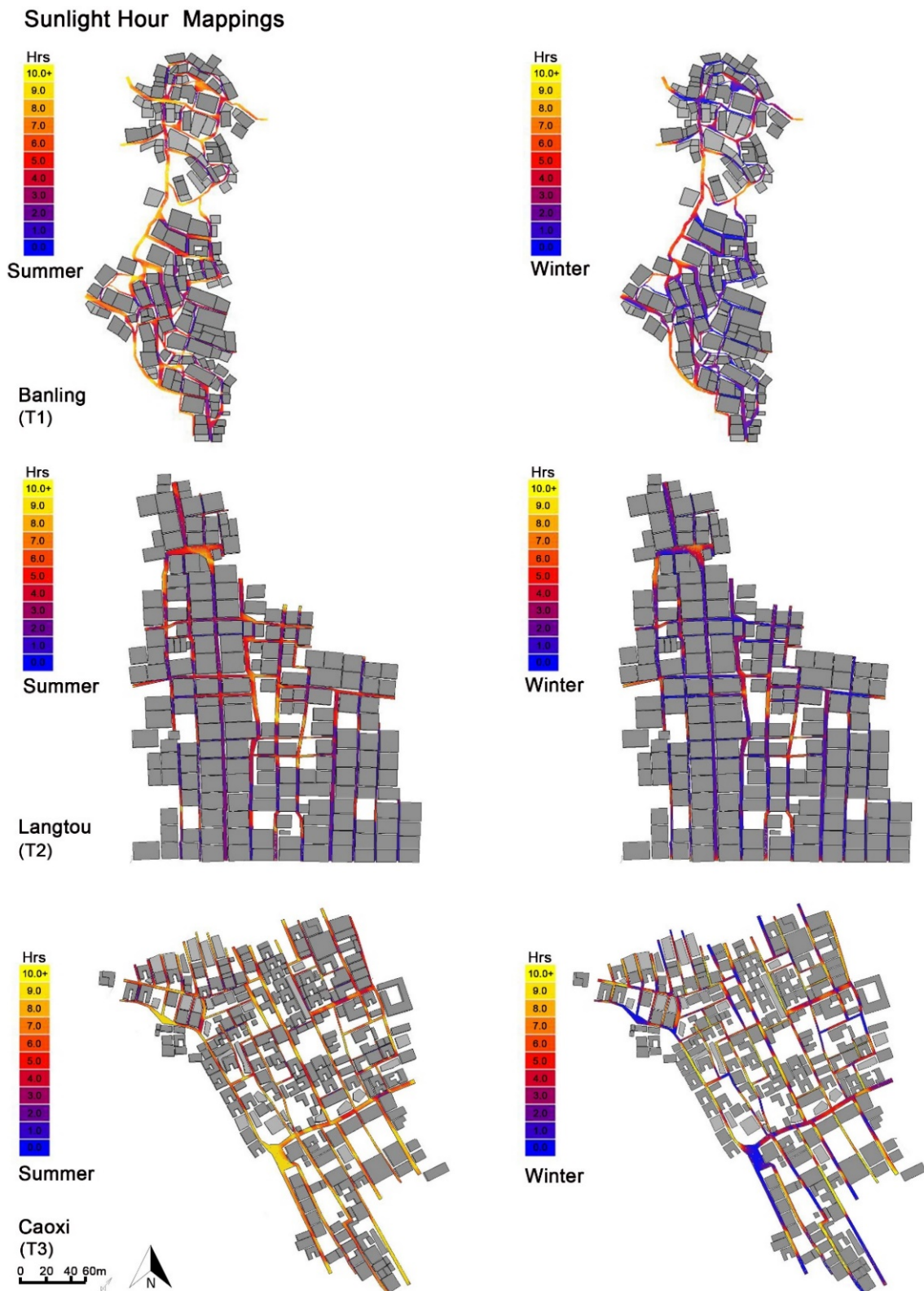


Figure 5. Total sunlight hour mappings of streets for wintertime and summertime for the three traditional settlements under study.

In the case of Langtou (T2), the analysis of SVF mapping indicates that low SVF between 0.10 and 0.20 and 0.21 and 0.40 cover 20% and 42.9% of the streetscape area, respectively (Table 5, Figure 4). This is due to the organized layout of buildings in Langtou

(T2), with closely connected building clusters and a predominant linear spatial arrangement. The street corridors in the settlement are long-narrow ($H/W = 1.9\sim 5.5$). This design approach, to some extent, increases the shading in local streetscapes and reduces incident solar radiation. The high SVF values in the ranges of 0.51–0.60 and 0.61–0.80, respectively, account for 10.1% and 9.8%. Analysis of sunlight hours received by the streetscape surfaces indicates that the streetscape shading rate is 62.4% in summer, which can somewhat reduce incident solar radiation and lower temperatures. In winter, the streetscape shading rate is 74.7% (Table 4, Figure 5).

In the case of Chaoxi (T3), the SVF mappings at the street level show that high SVF, which ranges from 0.40~0.80, accounts for 52.9% of the streetscape area (Table 5, Figure 4). This indicates that the majority of the settlement's streetscape has a relatively high SVF. This can be attributed to the presence of low-rise buildings and the semi-dispersed configuration of the settlement. In contrast, the low SVF range of 0.01 to 0.40 only covers 8.1% of the streetscapes area. High SVF values in the range of 0.81–0.90 and 0.91–1 accounted for 16.2% and 15.6% of the streetscapes area, respectively. In the widened streetscapes along the buildings, high SVF was simulated. In summer, most settlements' streetscapes are exposed to incident solar radiation, with a shading rate of only 28.4%, which provides an uncomfortable walking experience for pedestrians. In winter, the shading rises to 49.5% (Table 4, Figure 5).

This study, through surveys conducted in the three settlements, revealed that the lowest SVF occurred in Banling (T1), followed by Lantou (T2), and then Chaoxi (T3). Simulations confirmed that street corridors with low SVF would result in higher local shading. As a result, Banling (T1) had the highest shading ratio throughout the year, followed by Lantou (T2), and then Chaoxi (T3). In winter, most of the street corridors experience overshadowing, especially in Banling (T1). It is worth noting that, in the streetscape's high SVF values in Chaoxi (T3), widening the streetscape along the buildings can provide sufficient solar penetration capacity, thereby alleviating overshadowing during the winter. In summer, most of the streetscape in Banling (T1) can avoid intense incident solar radiation, while a significant proportion of the streetscape in Lantou (T2) also receives sufficient shading. In contrast, the shading effect along the street corridors is not ideal in Chaoxi (T3), due to some unshaded widening streetscapes.

3.4. Environmental Explanation of Streetscapes Based on Ventilation Simulation

Analyses of wind speed mappings indicate (Figure 6) that the wind speed of 0.7 m/s ~5.0 m/s accounts for 41% of the streetscape area. The maximum wind speed zone in Banling (T1) occurs at A-1, with a wind speed of 7 m/s~12 m/s, and the minimum wind speed zone occurs at A-2 with a wind speed of <0.7m/s. Ventilation street corridors are formed in A-S-1 and A-S-2, probably because street corridors are in the same direction as the prevailing wind and the continuous and narrow street corridors (S–N orientation) with small directional angles (<30°). In contrast, the occurrence of continuous large areas with wind speeds >5.0 m/s may be attributed to the constraints imposed by the mountainous terrain on the settlement, resulting in winding and meandering streets corridors. Additionally, the presence of certain buildings and street corridors with significant angles (>60°) relative to the prevailing wind direction could contribute to the formation of these high wind speed zones. More specially, under the influence of vertical wind direction, some areas of A-S-2, A2, and A1 may form three patterns of isolated bypass flow, mutual influence bypass flow, and glide flow, and include the "Street Canyon Effect" in the middle of the street and at the corners.

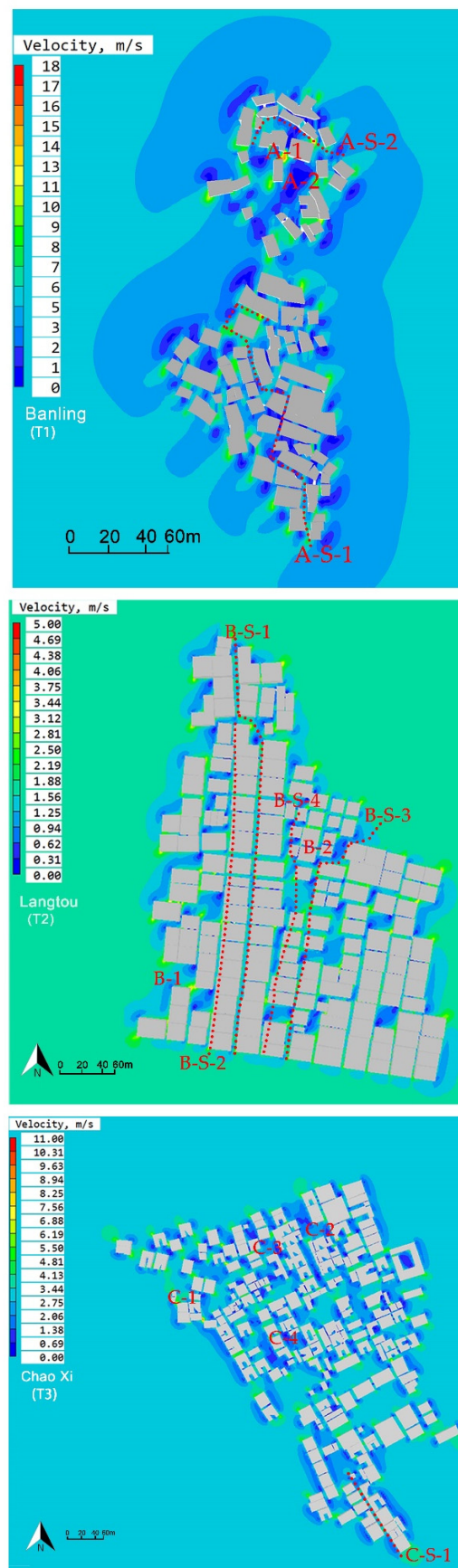


Figure 6. Wind speed mappings of streets for summertime for the three settlements under study.

The summer wind speed simulation results in Longtou (T2) show that the overall wind speed in the area is more desirable (Figure 6). The wind speed of 0.7 m/s~5.0 m/s accounts for 41% of the streetscape area. The maximum wind speed zone occurs at B-1, with wind speed reaching 5 m/s, and the minimum wind speed zone occurs at B-2, with almost no wind there during summer. Streets (B-S-1 and B-S-2) oriented in an N–S direction and parallel to the prevailing wind are susceptible to the narrow tube effect. The street structure is intersected by the NE–SW and SE–NW directions, resulting in a small internal ventilation environment. However, there are noticeable differences in ventilation conditions among various street corridors. For instance, the N–E direction of B-S-3 and B-S-4 exhibits lower wind speeds ranging from 0.31 m/s~0.94 m/s. This is attributed to the complex airflow penetrating internally and forming vortex airflow near B-S-3 and B-S-4. This phenomenon may be caused by wind paths with certain turns and street corridors intersecting the semi-enclosed space of the courtyard inside the settlement, as shown in the figure.

The simulation results of summer wind speeds in Chaoxi (T3) showed that the wind speed of 0.7 m/s~5.0 m/s accounts for 76% of the streetscape area (Figure 6). However, the overall air circulation within the settlement is poor, lacking continuous and interconnected “cool lanes”. The areas with higher wind speeds were mainly concentrated around the boundaries of the settlement, with the maximum wind speed occurring at C-1, with wind speed reaching 6 m/s~8.5 m/s. The gaps between buildings at the front and back edges of the settlement formed potential channels for the natural wind to enter the village (C-S-1). However, due to the opposite orientation of the settlement’s buildings to the prevailing southwest wind direction in summer, and the lack of appropriate wind channeling space planning, combined with the loosely arranged internal building layout and narrow and shallow streets, the external wind is unable to penetrate the public spaces within the settlement. As a result, a significant number of clam wind zones are generated within the settlement (c-2, c-3, and c-4). It is worth noting that the Leizhou Peninsula is a primary landing site for typhoons, and the enclosed spaces formed by residential courtyards can significantly enhance their wind and drainage resistance capabilities. The connected buildings around the periphery of the settlement and the loose alleys inside can also serve as barriers, reducing the possibility of the accommodation being damaged by typhoons.

This study, based on investigations of the ventilation environment in three settlements, reveals that the area with the highest proportion of pedestrian wind comfort is found in Longtou (T2), followed by Chaoxi (T3), and then Banling (T1). The simulation confirms that the buildings are densely arranged, and the street corridor openings are parallel to or form angles $<30^\circ$ with the dominant wind direction in summer. The overall layout of the streetscape is primarily oriented in NW–SE longitudinal street corridors, with SW–NE horizontal street corridors intersecting and intertwining with them. Additionally, by incorporating semi-enclosed streetscapes along the buildings within the settlement, it is easier to create internally interconnected “cool lanes”. In Banling (T1), the ventilation effect along the streets corridors is not ideal, mainly due to the constraints imposed by the mountainous conditions. The street corridors are winding and meandering, and certain buildings and street corridors have a large angle of deviation from the prevailing wind direction, resulting in dramatic variations in wind speed, while, in Chaoxi (T3), due to the intention of reducing typhoons’ negative impact, the overall architectural layout is loose, and the street corridors are shallow. As a result, it is not possible to form continuous natural ventilation corridors within the settlement’s interior spaces.

3.5. Environmental Explanation of Public Covered Streetscape

A comparative analysis of streetscapes’ insolation and ventilation environments in plain settlements with different H/W, and shaded and unshaded facilities was conducted. From the results of existing studies and data from field research, it can be found that the sample settlements have H/W ranging from 1 to 4 (streetscape height is determined by the

eaves and ridge heights of the buildings on both sides, with the relatively fixed building height as a constant value and the streetscape width as a variable.).

The results in Table 6 show that, as H/W increase, the obstructive effect of shading facilities on streetscapes decreases. This suggests that streetscapes with low H/W (i.e., high SVF) are more likely to be exposed to solar radiation, In contrast, those with high H/W (i.e., low SVF) can reduce solar radiation. As shown in Table 6, in summer, streetscapes with shading facilities and H/W in the range of 1–4 produce more additional shading (3.6–22%) compared to streetscapes without shading facilities. Regarding the ventilation environment, taking the street corridor with an S–E orientation as an example, they were divided into four groups for calculation. Table 7 shows that the wind speed at A1 and A3 are relatively stable, while the wind speed at A2 exhibits fluctuating undulations. The wind speed at A4 shows a rapid increase trend. When the H/W is equal to 1, the natural wind passing through the street corridors experiences a significant decrease in speed. When H/W is 3~4, the wind speed at the street entrance will experience a certain decrease. However, the wind speed variation in the middle and at the end of the street corridor remains relatively small, resulting in a higher level of pedestrian comfort.

Table 6. Mean monthly and mean seasonal additional shading contribution of covered over uncovered south–north-oriented street corridor for different H/W.

Additional Average Shade on a Horizontal Surface (%)				
	H/W = 1	H/W = 2	H/W = 3	H/W = 4
Winter	19	9	5	3
Dec	18	9	4	2
Jan	19	10	5	3
Feb	20	10	6	4
Spring	22	10	4.6	3
Mar	22	9	5	3
Apr	23	10	5	3
May	21	11	4	3
Summer	22	13	5.3	3.6
June	20	14	4	4
July	20	13	6	4
Aug	26	12	6	3
Autumn	20	10	4.6	2.6
Sept	21	10	5	3
Oct	21	10	4	2
Nov	18	10	5	3

Table 7. Wind speeds simulation for different H/W specifications.

Sample Number	Street Height–Width Ratios	Street Entrance Wind Speed (m/s)	Wind Speed in the Middle of the Street (m/s)	Wind Speed at the End of the Street (m/s)
A1	H/W = 1	2.3	2.9	3.2
A2	H/W = 2	4.1	3.3	4.3
A3	H/W = 3	3.2	3.3	4.0
A4	H/W = 4	2.9	3.3	4.0

4. Discussion

The comprehensive analysis of representative Lingnan traditional settlements in subtropical China indicates that different topographic features and architectural forms can result in variations in insolation and ventilation in the streetscape. Findings suggest that topographies significantly impact the spatial arrangement of street corridors and building massing configurations, particularly in mountainous regions. This finding is consistent with the conclusions of other scholars [35]. It indicates that the orientation, slope, and

natural landscape enclosure of the topography are essential factors affecting incident solar radiation and wind speed in the settlement [12,48]. Specifically, during the winter, traditional accommodations situated on the south-facing slopes can maximize their absorption of solar radiation. Settling in hilly river valleys with the back facing the mountains and the front facing the summer prevailing wind direction provides better ventilation conditions for the traditional settlement. Consistent with previous research findings, this study also found that, in addition to topographical factors, mountain-water pattern characteristics, building massing configurations, street corridor structure, and landscape configuration can also affect the solar radiation and wind speed in streetscapes [8]. In addition, simulation studies have also confirmed the previous research findings, demonstrating that compared to streetscapes with a low H/W distributed in loosely structured building layouts, those with a high H/W allocated in regular building layouts have higher shading rates and more comfortable ventilation conditions throughout the year [20].

The investigation results indicate that different building density configurations will result in varying shading patterns for traditional settlements located in coastal hills, plains, and mountainous regions. The building density configurations increase with the terrain's slope and the construction's difficulty. Due to geographical and available land area limitations, mountainous settlements have narrower, more varied, and more compact street corridor organization and a scattered and intertwined architectural spatial layout, with the highest shading rate (63.6%) in summer. Notably, traditional settlements in plains, with their "comb-like spatial layout," also exhibit a high shading rate of 62.4% during summer. The findings presented in this paper also supplement the conclusions of previous studies conducted by Jiafeng Weng [49]. Specifically, installing shading devices above street corridors has been shown to reduce solar radiation in summer. At the same time, it has been demonstrated that such covered street corridors do not generate excessive additional shading in winter. In addition, the overshadowing, particularly in mountainous areas, is also a concern during the winter. Findings suggest that overshadowing can be moderated by adjusting the building fabric and widening the streetscape.

Regarding ventilation conditions, the plain traditional settlement performs better than the traditional settlement in the mountains and coastal hills. The optimal ventilation performance of interior spaces within plain traditional settlements is attributed to a combination of factors, including the compact arrangement of buildings, alignment of building orientation and corridor direction with the prevailing summer winds, a high H/W, semi-enclosed open courtyards, and site-specific landscape configurations. Figure 6 indicates that the overall wind environment is favorable in the periphery of the mountainous traditional settlement. The settlement is located in a canyon area, with tall mountains to the west and hills to the north. The open areas to the east and south and at a distance from the hills to the east, can block the cold winter winds while welcoming the cool summer breeze. However, the ventilation conditions within mountainous settlements are not ideal, primarily due to the changes in street layout caused by the topography. This can result in local areas where the angle between the corridors and the prevailing wind direction becomes excessively large, even approaching 90°, which is unfavorable for ventilation. In the summer, coastal hill traditional settlements built on gently sloping peninsulas benefit from good ventilation because the peripheral buildings (in the southeast direction) are connected and oriented parallel to the prevailing wind direction. This, combined with plant enclosures and water features, creates a micro-environment conducive to ventilation. However, due to the lack of corresponding wind guidance planning within the settlement, the loose building layout and the low H/W fail to draw the surrounding winds further into the settlement's interior space. This is because the region is prone to typhoons, and such a building layout can help resist them and accelerate drainage. The simulation results of Table 7 indicate that the H/W = 3~4 can effectively improve ventilation conditions.

5. Conclusions

The novelty of this study is the investigation and evaluation of insolation and ventilation conditions in traditional settlement streetscapes in different topographical and climatic zones. It explores the transfer of knowledge from the traditional passive design approaches to the climate-responsive design strategies of modern urban outdoor spaces and the potential for improving existing streetscape thermal comfort. It also presents an analytical method based on the comparative evaluation of environment variables at different sites. The research results will apply to other regions with subtropical climate characteristics, especially in coastal hilly areas, plains, and mountainous regions. The improvements in future research will include the use of higher-resolution satellite data and other thermal comfort variables such as air humidity, physiological equivalent temperature (PET), and wind pressure to study the synergistic effects of these variables. This will achieve more accurate simulation results and precise mapping for specific locations. Within the accurate range allowed by the selected data sources, this study confirms that the passive design approaches of traditional settlements can provide valuable knowledge and inspiration. It has a practical significance in providing recommendations for urban-outdoor-space climate-responsive design strategies and environmental policies.

More specifically:

- (1) The unique topographic characteristics of settlement locations, such as orientation, elevation, and slope, have a significant impact on incident solar radiation. It is recommended that settlement sites with an average elevation of 600 m be located on southeast-facing slopes with slopes ranging from 10° ~ 20° . Compared to a gentle terrain, this inclination can provide an additional 10% of incident solar radiation, thus increasing incident solar radiation during winter.
- (2) In summer, the comb-shaped architectural spatial layout of settlements on plains, with long-narrow street corridors ($H/W = 1.9\sim 5.5$) oriented in the NE–SW longitudinal, can result in a low SVF of 62.9% and 62% shading ratio. However, these spaces require the implementation of deciduous tree planting or sun-shading devices fixed on horizontal surfaces along the street corridors to reduce incident solar radiation during the summer.
- (3) Installing shading facilities along the horizontal surfaces of covered street corridors is considered to be the most effective measure for enhancing additional shading in streetscapes and reducing incident solar radiation during the summer. Based on the simulation, compared to a $H/W = 4$, which provides an additional shading of 3.6%, this spatial configuration in a $H/W = 1$ can achieve an additional shading of 22%.
- (4) Improving pedestrian comfort with wind speeds in streetscapes requires attention to the following factors: (i) Settlement sites in mountainous areas are preferably located in hilly river valleys. These sites are situated on slopes adjacent to water bodies or on flat terrains near mountain passes, which helps to avoid the intense airflow variations on mountaintops and the calm wind zones in low-lying areas. (ii) In plains settlements, creating a favorable external ventilation environment can be achieved by positioning water bodies or open spaces at the periphery of buildings, aligned with the dominant wind direction during the summer. Additionally, enclosing these areas by planting trees can further enhance ventilation. (iii) The following measures can help improve the ventilation environment within the settlement: Creating a compact arrangement of buildings with a $H/W = 3\sim 4$ is beneficial for improving the internal ventilation environment within a settlement. The main street, oriented towards the dominant wind direction in summer, should form an angle of $<30^{\circ}$ with it. The primary street corridors should follow a NE–SW longitudinal orientation, serving as the main thoroughfare, while SE–NW-oriented horizontal street corridors should intersect and weave through it, forming a grid-like pattern of the streetscape. Expanding the streetscape along the buildings allows for the introduction of wind into the interior of the settlement. For coastal hilly areas, low-rise buildings, internally

dispersed building layouts, and a $H/W = 0.9\sim 2.3$ can help mitigate the typhoons' negative impacts.

In conclusion, research indicates that traditional settlements achieve low energy consumption for thermal comfort and create favorable microclimate conditions by implementing passive design approaches and concepts that bridge the gap between buildings and the natural environment. This is particularly evident in the case of settlements in plains. For that reason, we believe that vernacular architecture can be transformed into a powerful design database to identify, enhance, and evolve architectural forms that promote thermal comfort in particular regions. In the future, it is worth researching other spatial characteristics of urban areas, such as traditional building courtyards, building envelopes, and architectural typologies. Researchers can revisit traditional passive design concepts to improve the thermal comfort of outdoor spaces in a broader range of geographical and climatic contexts. This will provide inspiration and recommendations for developing climate-responsive design strategies and environmental planning policies for contemporary urban outdoor spaces.

Author Contributions: Conceptualization, Y.L. (Yalun Lei) and Q.L.; methodology, H.Z.; software, Y.L. (Yigang Liu); validation, J.L. and C.W.; formal analysis, Y.L. (Yalun Lei); investigation, C.W.; resources, Q.L.; data curation, Y.L. (Yigang Liu); writing—original draft preparation, Y.L. (Yalun Lei); writing—review and editing, H.Z.; supervision, Y.L. (Yalun Lei); funding acquisition, Y.L. (Yalun Lei). All authors have read and agreed to the published version of the manuscript.

Funding: This research was funded by the Office of the Leading Group for Shanghai Art Science Planning (2022 Shanghai Art Science Planning Project, Grant number: YB2022-F-088).

Data Availability Statement: The data used to support the findings of this study are included in the article.

Conflicts of Interest: The authors declare that they have no conflict of interest or personal relationships that could have appeared to influence the work reported in this paper.

References

1. Zhang, X.; Wang, Y.; Zhou, D.; Yang, C.; An, H.; Teng, T. Comparison of Summer Outdoor Thermal Environment Optimization Strategies in Different Residential Districts in Xi'an, China. *Buildings* **2022**, *12*, 1332. [[CrossRef](#)]
2. Slorach, P.C.; Stamford, L. Net Zero in the Heating Sector: Technological Options and Environmental Sustainability from Now to 2050. *Energy Convers. Manag.* **2021**, *230*, 113838. [[CrossRef](#)]
3. Mostafavi, F.; Tahsildoost, M.; Zomorodian, Z. Energy Efficiency and Carbon Emission in High-Rise Buildings: A Review (2005–2020). *Build. Environ.* **2021**, *206*, 108329. [[CrossRef](#)]
4. Fan, W.; Zhang, J.; Zhou, J.; Li, C.; Hu, J.; Hu, F.; Nie, Z. LCA and Scenario Analysis of Building Carbon Emission Reduction: The Influencing Factors of the Carbon Emission of a Photovoltaic Curtain Wall. *Energies* **2023**, *16*, 4501. [[CrossRef](#)]
5. Rogelj, J.; Geden, O.; Cowie, A.; Reisinger, A. Net-Zero Emissions Targets Are Vague: Three Ways to Fix. *Nature* **2021**, *591*, 365–368. [[CrossRef](#)] [[PubMed](#)]
6. Xu, G.; Wang, W. China's Energy Consumption in Construction and Building Sectors: An Outlook to 2100. *Energy* **2020**, *195*, 117045. [[CrossRef](#)]
7. Nawrath, M.; Kowarik, I.; Fischer, L.K. The Influence of Green Streets on Cycling Behavior in European Cities. *Landsc. Urban Plan.* **2019**, *190*, 103598. [[CrossRef](#)]
8. Xiong, Y.; Zhang, J.; Yan, Y.; Sun, S.; Xu, X.; Higuera, E. Effect of the Spatial Form of Jiangnan Traditional Villages on Microclimate and Human Comfort. *Sustain. Cities Soc.* **2022**, *87*, 104136. [[CrossRef](#)]
9. Lei, Y.; Zhou, H.; Wang, M.; Wang, C. Analysis on Spatial Characteristics and the Adaptation Mechanism of Miao Traditional Settlement in Qiandongnan, China. *Math. Probl. Eng.* **2022**, *2022*, 6293833. [[CrossRef](#)]
10. Kaihou, A.; Sriti, L.; Amraoui, K.; Di Turi, S.; Ruggiero, F. The Effect of Climate-Responsive Design on Thermal and Energy Performance: A Simulation Based Study in the Hot-Dry Algerian South Region. *J. Build. Eng.* **2021**, *43*, 103023. [[CrossRef](#)]
11. de Dear, R.; Xiong, J.; Kim, J.; Cao, B. A Review of Adaptive Thermal Comfort Research since 1998. *Energy Build.* **2020**, *214*, 109893. [[CrossRef](#)]
12. Yang, W.; Xu, J.; Lu, Z.; Yan, J.; Li, F. A Systematic Review of Indoor Thermal Environment of the Vernacular Dwelling Climate Responsiveness. *J. Build. Eng.* **2022**, *53*, 104514. [[CrossRef](#)]
13. Nguyen, A.T.; Truong, N.S.H.; Rockwood, D.; Tran Le, A.D. Studies on Sustainable Features of Vernacular Architecture in Different Regions across the World: A Comprehensive Synthesis and Evaluation. *Front. Archit. Res.* **2019**, *8*, 535–548. [[CrossRef](#)]

14. Osman, M.M.; Sevinc, H. Adaptation of Climate-Responsive Building Design Strategies and Resilience to Climate Change in the Hot/Arid Region of Khartoum, Sudan. *Sustain. Cities Soc.* **2019**, *47*, 101429. [CrossRef]
15. Du, Y.; Zhu, Z. Research on the Form of Energy-Saving Building under the Influence of Natural Ventilation Technology. *J. Phys. Conf. Ser.* **2023**, *2468*, 012163. [CrossRef]
16. Hu, M.; Zhang, K.; Nguyen, Q.; Tasdizen, T. The Effects of Passive Design on Indoor Thermal Comfort and Energy Savings for Residential Buildings in Hot Climates: A Systematic Review. *Urban Clim.* **2023**, *49*, 101466. [CrossRef]
17. Yang, L.; Fu, R.; He, W.; He, Q.; Liu, Y. Adaptive Thermal Comfort and Climate Responsive Building Design Strategies in Dry–Hot and Dry–Cold Areas: Case Study in Turpan, China. *Energy Build.* **2020**, *209*, 109678. [CrossRef]
18. Cui, L.; Wang, J.; Sun, L.; Lv, C. Construction and Optimization of Green Space Ecological Networks in Urban Fringe Areas: A Case Study with the Urban Fringe Area of Tongzhou District in Beijing. *J. Clean. Prod.* **2020**, *276*, 124266. [CrossRef]
19. Jiang, Y.; Song, D.; Shi, T.; Han, X. Adaptive Analysis of Green Space Network Planning for the Cooling Effect of Residential Blocks in Summer: A Case Study in Shanghai. *Sustainability* **2018**, *10*, 3189. [CrossRef]
20. Aboelata, A. Vegetation in Different Street Orientations of Aspect Ratio (H/W 1:1) to Mitigate UHI and Reduce Buildings' Energy in Arid Climate. *Build. Environ.* **2020**, *172*, 106712. [CrossRef]
21. Xie, H.; Huang, T.; Li, J.; Liu, J.; Niu, J.; Mak, C.M.; Lin, Z. Evaluation of a Multi-Nodal Thermal Regulation Model for Assessment of Outdoor Thermal Comfort: Sensitivity to Wind Speed and Solar Radiation. *Build. Environ.* **2018**, *132*, 45–56. [CrossRef]
22. Yıldırım, M. Shading in the Outdoor Environments of Climate-Friendly Hot and Dry Historical Streets: The Passageways of Sanliurfa, Turkey. *Environ. Impact Assess. Rev.* **2020**, *80*, 106318. [CrossRef]
23. Patandianan, M.V.; Shibusawa, H. Importance and Performance of Streetscapes at a Tourism Destination in Indonesia: The Residents' Perspectives. *Front. Archit. Res.* **2020**, *9*, 641–655. [CrossRef]
24. Cui, P.; Jiang, J.; Zhang, J.; Wang, L. Effect of Street Design on UHI and Energy Consumption Based on Vegetation and Street Aspect Ratio: Taking Harbin as an Example. *Sustain. Cities Soc.* **2023**, *92*, 104484. [CrossRef]
25. Ge, J.; Wang, Y.; Akbari, H.; Zhou, D. The Effects of Sky View Factor on Ground Surface Temperature in Cold Regions—A Case from Xi'an, China. *Build. Environ.* **2022**, *210*, 108707. [CrossRef]
26. Antoniadis, D.; Katsoulas, N.; Kittas, C. Simulation of Schoolyard's Microclimate and Human Thermal Comfort under Mediterranean Climate Conditions: Effects of Trees and Green Structures. *Int. J. Biometeorol.* **2018**, *62*, 2025–2036. [CrossRef] [PubMed]
27. Jiang, Y.; Han, X.; Shi, T.; Song, D. Microclimatic Impact Analysis of Multi-Dimensional Indicators of Streetscape Fabric in the Medium Spatial Zone. *Int. J. Environ. Res. Public Health* **2019**, *16*, 952. [CrossRef] [PubMed]
28. Sarkar, A.; Bardhan, R. Socio-Physical Liveability through Socio-Spatiality in Low-Income Resettlement Archetypes—A Case of Slum Rehabilitation Housing in Mumbai, India. *Cities* **2020**, *105*, 102840. [CrossRef]
29. Huang, J.; Jones, P.; Zhang, A.; Peng, R.; Li, X.; Chan, P. Urban Building Energy and Climate (UrBEC) Simulation: Example Application and Field Evaluation in Sai Ying Pun, Hong Kong. *Energy Build.* **2020**, *207*, 109580. [CrossRef]
30. Lai, D.; Liu, W.; Gan, T.; Liu, K.; Chen, Q. A Review of Mitigating Strategies to Improve the Thermal Environment and Thermal Comfort in Urban Outdoor Spaces. *Sci. Total Environ.* **2019**, *661*, 337–353. [CrossRef]
31. Jiang, Y.; Wu, C.; Teng, M. Impact of Residential Building Layouts on Microclimate in a High Temperature and High Humidity Region. *Sustainability* **2020**, *12*, 1046. [CrossRef]
32. Galal, O.M.; Sailor, D.J.; Mahmoud, H. The Impact of Urban Form on Outdoor Thermal Comfort in Hot Arid Environments during Daylight Hours, Case Study: New Aswan. *Build. Environ.* **2020**, *184*, 107222. [CrossRef]
33. Philokyprou, M.; Michael, A. Environmental Sustainability in the Conservation of Vernacular Architecture. The Case of Rural and Urban Traditional Settlements in Cyprus. *Int. J. Archit. Herit.* **2021**, *15*, 1741–1763. [CrossRef]
34. Hegazy, I.R.; Qurnfulah, E.M. Thermal Comfort of Urban Spaces Using Simulation Tools Exploring Street Orientation Influence of on the Outdoor Thermal Comfort: A Case Study of Jeddah, Saudi Arabia. *Int. J. Low-Carbon Technol.* **2020**, *15*, 594–606. [CrossRef]
35. Hermawan, H.; Švajlenka, J. Building Envelope and the Outdoor Microclimate Variable of Vernacular Houses: Analysis on the Environmental Elements in Tropical Coastal and Mountain Areas of Indonesia. *Sustainability* **2022**, *14*, 1818. [CrossRef]
36. Zhang, Y. Study on Energy-Saving Thermal Environment of Residential Envelope Reconstruction Based on ECOTECH. In Proceedings of the International Conference on Smart Transportation and City Engineering, Chongqing, China, 26–28 October 2021; Volume 12050, pp. 805–809.
37. Chinese Lighting Design Standard. Available online: <https://www.chinesestandard.net/PDF.aspx/GB50034-2013> (accessed on 18 June 2023).
38. National Meteorological Information Center. Available online: <https://data.cma.cn/data/> (accessed on 16 May 2023).
39. Bai, L.; Wang, S. Definition of New Thermal Climate Zones for Building Energy Efficiency Response to the Climate Change during the Past Decades in China. *Energy* **2019**, *170*, 709–719. [CrossRef]
40. Guo, P.; Ding, C.; Guo, Z.; Liu, T.; Lyu, T. Coupling CFD Simulation and Field Experiments in Summer to Prove Feng Shui Optimizes Courtyard Wind Environments: A Case Study of Prince Kung's Mansion in Beijing. *Buildings* **2022**, *12*, 629. [CrossRef]
41. Li, Y.; Chen, L.; Yang, L. CFD Modelling and Analysis for Green Environment of Traditional Buildings. *Energies* **2023**, *16*, 1980. [CrossRef]
42. Ma, H.; Zhou, X.; Tominaga, Y.; Gu, M. CFD Simulation of Flow Fields and Pollutant Dispersion around a Cubic Building Considering the Effect of Plume Buoyancies. *Build. Environ.* **2022**, *208*, 108640. [CrossRef]

43. Ying, X.; Wang, Y.; Li, W.; Liu, Z.; Ding, G. Group Layout Pattern and Outdoor Wind Environment of Enclosed Office Buildings in Hangzhou. *Energies* **2020**, *13*, 406. [[CrossRef](#)]
44. Li, W.; Ye, H.; Wang, Q.; Liu, H.; Ding, T.; Liu, B. Experimental Study on the Seismic Performance of Demountable RCS Joints. *J. Build. Eng.* **2022**, *49*, 104082. [[CrossRef](#)]
45. Xiong, M.; Chen, B.; Zhang, H.; Qian, Y. Study on Accuracy of CFD Simulations of Wind Environment around High-Rise Buildings: A Comparative Study of $k-\epsilon$ Turbulence Models Based on Polyhedral Meshes and Wind Tunnel Experiments. *Appl. Sci.* **2022**, *12*, 7105. [[CrossRef](#)]
46. Ying, X.; Qin, X.; Shen, L.; Yu, C.; Zhang, J. An Intelligent Planning Method to Optimize High-Density Residential Layouts Considering the Influence of Wind Environments. *Heliyon* **2023**, *9*, e13051. [[CrossRef](#)]
47. Zhen, M.; Chen, Z.; Zheng, R. Outdoor Wind Comfort and Adaptation in a Cold Region. *Buildings* **2022**, *12*, 476. [[CrossRef](#)]
48. Nie, Q.; Zhao, S.; Zhang, Q.; Liu, P.; Yu, Z. An Investigation on the Climate-Responsive Design Strategies of Vernacular Dwellings in Khams. *Build. Environ.* **2019**, *161*, 106248. [[CrossRef](#)]
49. Lam, C.K.C.; Weng, J.; Liu, K.; Hang, J. The Effects of Shading Devices on Outdoor Thermal and Visual Comfort in Southern China during Summer. *Build. Environ.* **2023**, *228*, 109743. [[CrossRef](#)]

Disclaimer/Publisher's Note: The statements, opinions and data contained in all publications are solely those of the individual author(s) and contributor(s) and not of MDPI and/or the editor(s). MDPI and/or the editor(s) disclaim responsibility for any injury to people or property resulting from any ideas, methods, instructions or products referred to in the content.